Research Article

iMedPub Journals
www.imedpub.com

Journal of Clinical Pathology and Diagnosis

2018
Vol.1 No. 1:4

Preliminary Histopathologic Study on a Reciprocal Relationship Between Spinal Deformity and a Triad of Intervertebral Disc, Spinal Cord and Skeletal Muscle in Swine

Ohfuji S*

Department of Histopathology, Diagnostic Animal Pathology Office, Hokkaido, Japan

***Corresponding author:**
Ohfuji S

ssmohfuji@yc5.so-net.ne.jp

Department of Histopathology, Diagnostic Animal Pathology Office, Hokkaido, Japan.

Tel: +81116717118
Fax: +81116717118

Citation: Ohfuji S (2018) Preliminary Histopathologic Study on a Reciprocal Relationship Between Spinal Deformity and a Triad of Intervertebral Disc, Spinal Cord and Skeletal Muscle in Swine. J Clin Pathol Diagn Vol.1 No.1:4

Abstract

Background: Knowledge of spinal deformity in swine remains still fluxional. Although pathologic reports of swine cases with neuromuscular spinal deformity are scarce, it is important to elucidate from the comparative viewpoint whether the development of spinal deformity in pigs is correlated with pathology of the spinal cord and/or skeletal muscle. In addition, intervertebral disc degeneration may be a complex process, but structural changes occurring in the deteriorated disc tissue is not fully explored.

Methods and findings: To evaluate a reciprocal relationship between spinal deformity and a triad of intervertebral disc, spinal cord, and skeletal muscle, a preliminary histopathologic study was conducted on 6 pigs (6 months of age) with thoracic kyphosis (1 case), lordokyphosis (1 case), or lordosis (4 cases). Annulus fibrosus between deformed vertebral bodies showed degeneration characterized by the occurrence of varying degrees of microcyst-like spaces, giving rise to an appearance of microcavitation or microporosity (6 cases). Focal necrosis was recognized in the annular matrix (4 cases). Chondrocytes showed positive labeling with the TUNEL assay, indicating apoptosis (6 cases). In addition, thoracic and lumbar segments of the spinal cord exhibited a minor extent of myelinated nerve fiber degeneration with no specific tract involvement in the white matter (6 cases). The muscle overlying the deformed spinal column had no significant changes.

Conclusions: Determining whether the structural changes observed in the annulus fibrosus played a primary role in the development of vertebral deformity or were secondary to mechanical overlord generated by the spinal deformity would require further investigation of deformed vertebral bodies. It is likely that myelinated nerve fiber alteration in the spinal cord was correlated with spinal deformity that gave mechanical damage to the spinal cord. The histopathologic findings observed in this small study may serve as a reference when studying deformities of the thoracic spinal column in humans.

Keywords: Annulus fibrosus; Apoptosis; Chondrocytes; Disc degeneration; Skeletal muscle; Spinal cord; Swine

Received: November 27, 2017; **Accepted:** January 05, 2018; **Published:** January 08, 2018

Introduction

Spinal deformity referred to as kyphosis, lordosis, or scoliosis is a well-known condition that afflicts humans [1-9]. This condition also involves domestic pigs worldwide [10-13]. An association with a variety of risk factors has been proposed, including developmental malformations, traumatic lesion, inflammation, metabolic bone disease, or abnormal body posture [7]. Some researchers reported that kyphosis condition in pigs is not associated with neurologic problems, metabolic diseases,

inflammation, or spinal infections [11]. Thus, knowledge of spinal deformity in this species remains still in a fluxional stage.

Studies have indicated that spinal cord injury in children may cause neuromuscular spinal deformity [14]. Neuromuscular spinal deformity is a condition that implies progressive spinal deformity associated with neuromuscular disorders, including Parkinson disease, cerebral palsy, multiple sclerosis, myelomeningocele, and myopathy [1,14,15]. To the best of the author's knowledge, pathologic reports of swine cases with neuromuscular spinal deformity are scarcely published in the veterinary literature perhaps because no disease like it has been recognized in this species. From the comparative viewpoint, it is of importance to elucidate whether the development of spinal deformity in pigs is correlated with pathology of the spinal cord and/or skeletal muscle overlying the spinal column.

There is a close relationship between spinal deformity and pathology of the intervertebral disc (IVD). In human patients with scoliosis, for example, some authors described that a highly organized elastic fiber network of IVD is sparse and disrupted, and such disorganized elastic fiber network is involved in the progression of spinal deformity [16]. Other authors found in scoliotic patients changes of disc cell degeneration or necrosis [2]. Degeneration of IVD may be a complex process characterized by highly intercorrelated biomechanical, biochemical, and cellular interactions, though, structural changes occurring in the deteriorated disc tissue matrix is not fully explored [17]. In dogs of nonchondrodystrophoid breeds, in which diseases involving the IVD may occur later in life, IVD degeneration histologically takes the form of necrosis [18], while in other domestic animal species including pigs, those published reports describing detailed histopathologic changes in IVD degeneration appear to be limited to a small number.

To evaluate a reciprocal relationship between spinal deformity and a triad of IVD, spinal cord, and skeletal muscle, a preliminary histopathologic study was conducted on pigs with thoracic column deformity.

Methods

Six pigs (Case Nos. 1-6) with spinal deformity and 6 control pigs, which had been fattened at different farms, were used for the study. All animals, 6 months old, were female Landrace crossbred pigs. Animals' histories and environmental conditions under which they were raised were unavailable. The pigs did not show neurologic deficits or other significant clinical signs at antemortem physical inspection, and were slaughtered at an abattoir on separate days over a 5-month period. The animals were electrically stunned and killed by exsanguination. After removal of the internal viscera and severing of the head depending on the slaughter process, the entire length of spinal column was cut mid-sagittally by using an electric sawing machine. When the animals were diagnosed as having deformed spinal column, as many IVDs as possible were immediately removed from the thoracic vertebral column with a scalpel. Approximately two-thirds of the annulus fibrosus (AF) and a small piece of outer zones of the nucleus pulposus (NP) were available for histopathologic examination because approximately one-third of the AF and large parts of the NP were lost at a time when the vertebral column was divided into halves. One pig (No. 3) had fusion of the thoracic vertebrae (synostosis) at the 7th and 8th level and at the 9th and 10th level, making it impossible to sample IVDs between these fused vertebral bodies. Thoracic and lumbar segments of the spinal cord and the longissimus thoracis muscle were taken for examination.

Tissue samples from 6 pigs with spinal deformity and from 6 unaffected control animals were fixed in 10% buffered formalin. After fixation, transverse tissue sections of each AF were processed by using standard histopathologic methods. Transverse sections of spinal cord and transverse/longitudinal sections of muscle were likewise processed. Paraffin-embedded sections were cut at 4 µm in thickness and stained with hematoxylin and eosin (HE). Selected sections were stained with periodic acid-Schiff (PAS), toluidine blue, elastica van Gieson (EVG), Von Kossa, and luxol fast blue (LFB)-HE methods. Immunohistochemical investigation was performed by a streptavidin-biotin-peroxidase complex method (Histofine SAB-PO kit; Nichirei Corp., Tokyo, Japan), according to the instructions provided by the manufacturer. The primary antibody used was rabbit polyclonal antibody against myelin basic protein (MBP, Nichirei, polyclonal rabbit, prediluted). Immunoreactivity was visualized using 3, 3'-diaminobenzidine-tetrahydrochloride as chromogen, and the sections were counterstained with Mayer's hematoxylin. For *in situ* detection of DNA strand breaks, *in situ* TUNEL (terminal deoxynucleotidyl transferase-mediated deoxyuridine triphosphate nick end-labeling) staining was applied on selected sections. An *in situ* Apoptosis Detection kit (Takara Biomedicals, Shiga, Japan) was used for the TUNEL assay. According to the manufacturer's instructions, tissue sections were covered with the TUNEL reaction mixture containing the terminal deoxynucleotidyl transferase. Then anti-fluorescein isothiocyanate (FITC)-streptavidin- horseradish-peroxidase (HRP) conjugate was added to each slide. Color development was performed with 3,3'-diaminobenzidine chromogen. The slides were counterstained with 3% methyl green.

Results

As given in **Table 1**, deformity of the thoracic spinal column, either kyphosis (case No. 1), lordokyphosis (case No. 2), or lordosis (case Nos. 3-6), was diagnosed during carcass inspection at slaughter **(Figure 1)**. IVD tissues between such deformed thoracic vertebrae exhibited, to varying degrees, the presence of small linear areas having a light brown discoloration in the AF of all pigs. These discolored areas were demonstrated in parallel to the horizontal axis of the concentric layers of AF.

Histopathologic findings in the IVD tissues included 3 main lesions in the AF; one was microcavitation or microporosity formation in all pigs, another, focal necrosis in 4 pigs, and the third, apoptosis of chondrocytes in all pigs. First, the AF of all 6 pigs exhibited degeneration characterized by the presence of a varying degree of clearly delineated microcyst-like spaces, giving rise to a microporous or microvacuolar appearance **(Figure 2)**. These spaces were detected in 40 of 77 (52%) of the examined AFs, consisting of 23 (95.8%) of 24 AFs from deformed spinal regions and 17 (32%) of 53 AFs from intact spinal regions. Lesions

Table 1 Gross findings in the thoracic spinal column and histopathologic findings in the annulus fibrosus of 6 pigs (Case no's. 1-6) and age-matched control pigs (Case no's. 7-12).

Case No.	Deformity of the spinal column	Histopathologic lesion[a] in the anuulus fibrosus of the thoracic vertebral column													
		T1-2	T2-3	T3-4	T4-5	T5-6	T6-7	T7-8	T8-9	T9-10	T10-11	T11-12	T12-13	T13-14	T14-15	T15-16
1	Kyphosis (T9-11)	-	-	-	-	-	n/a	+	+	+[b]	++[b]	+	-	-	n/a	-
2	Lordokyphosis (T7-16)	-	+	n/a	+	+	-	-	+	+	+	n/a	+	++[b]	++	+
3	Lordosis (T6-11)	-	-	-	+	+	n/a	n/a	+[b]	n/a	+	+	+	+	++	-
4	Lordosis (T5-12)	-	-	-	-	+	+	+	+	+	+	+	n/a	-	-	-
5	Lordosis (T5-9)	-	n/a	-	-	+	+	+	+[b]	+ [b]	n/a	-	-	-	-	-
6	Lordosis (T5-8)	-	-	-	-	n/a	+	n/a	+	+	+	+	-	-	n/a	-
7-12	No deformity	-	-	-	-	-	-	-	-	-	-	-	-	-	-	-

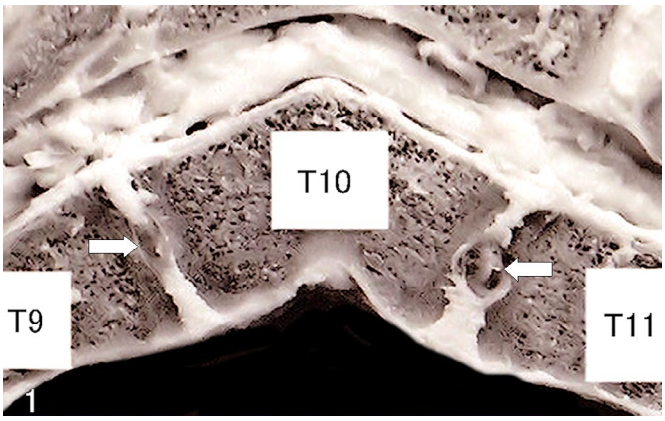

Figure 1 Case No. 1. Mid-sagittal cut surface of the kyphotic thoracic spinal column shows wedge-shaped curvature of the 10th thoracic vertebral body (T10). The intervertebral discs are grossly unremarkable. The nucleus pulposus of the intervertebral disc is almost lost (white arrows) at the time of mid-sagittal cutting of the spinal column.

of such microcavitation were more prominent in those concentric layers that were oriented at the same, rather than the alternative, angle. In many instances the microcyst-like spaces ranged in number between 10 and 30 per 40x field, while several AFs of 3 pigs (case Nos. 1-3) had more than 80 spaces per the same power field **(Table 1)**. Some spaces had a larger size (approximately 110 µm in diameter) than many others (<45 µm in diameter). No lining cells were seen in these spaces. Occasionally, coalescing features were present. Many microcyst-like spaces were empty, whereas some contained a small to moderate amount of fibrillary, string-like, or amorphous materials. The latter stained basophilic with HE, negative with PAS, orthochromatic with toluidine blue, and purplish black with EVG, indicating elastic tissue elements **(Figure 2, inset)**. Such elastic tissue elements within the spaces were either observed in a free state or adhered to the tissue pieces exfoliated from the annular matrix. These tissue pieces stained weakly eosinophilic with HE, pink with PAS, orthochromatic with toluidine blue, and reddish with EVG, indicating collagenous tissue elements. Second, in the annular matrix of 4 pigs (case Nos. 1-3, 5), there were variably sized necrotic foci ranging from approximately 210 to 400 µm in diameter. The incidence rate was 2 to 4 per 40x field, involving 1 to 2 AFs per animal **(Table 1)**. Focal necrotic lesions were characterized by well-delineated, hypereosinophilic areas comprised of pyknotic nuclei-like, nuclear debris-like, or dust-like substances and large amounts of fibrillary

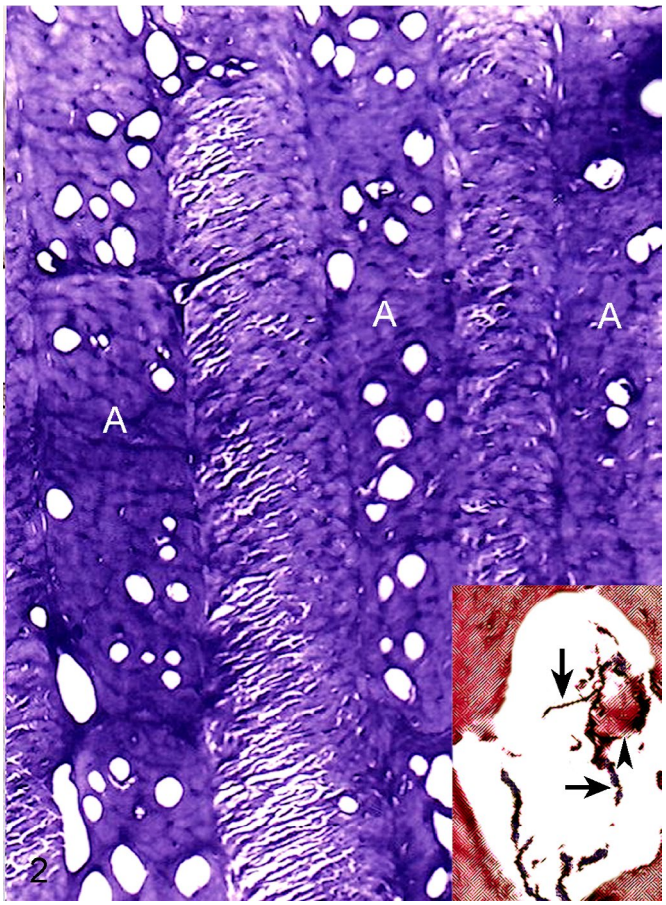

Figure 2 Annulus fibrosus. Transverse section exhibits an appearance of microcavitation characterized by a large number of microcyst-like spaces in the annulus fibrosus matrix. This microporous change is more remarkable in the concentric layers oriented at the same angle (A). Toluidine blue. Inset: The string-like or fibrillary materials (arrows) that stained purplish black adhere to exfoliated tissue piece (arrowhead) within a microcyst-like space. Elastica van Gieson.

to hyalinized materials indicative of necrotic collagen fibers **(Figure 3)**. The dust-like substances stained negatively for calcium salts with Von Kossa method. The matrix tissue surrounding necrotic foci had a poorly organized architecture. There were no cellular reactions against necrotic lesions. Third, many chondrocytes exhibiting chromatin-condensed or pyknotic nuclei and cytoplasmic shrinkage, with or without single cytoplasmic

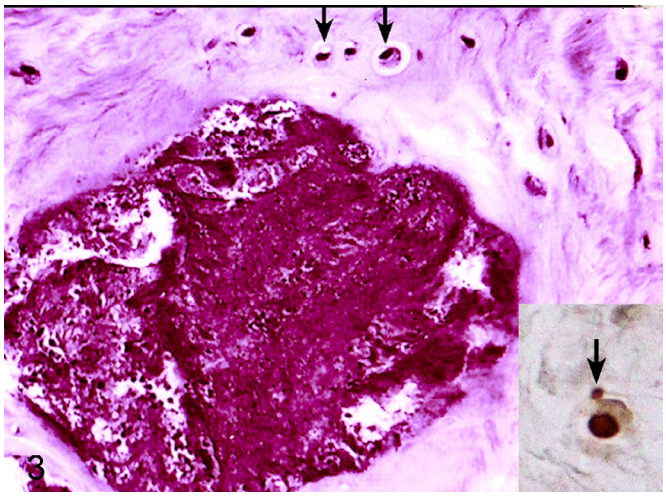

Figure 3 Annulus fibrosus. Focal necrosis shows hypereosinophilic amorphous area containing many granular materials indicative of nuclear debris. Chondrocytes (arrows) around the necrotic area show pyknotic nuclei. Hematoxylin and eosin (HE). Inset: Chondrocyte nucleus exhibits TUNEL positivity, and apoptotic body (arrow) is seen. TUNEL stain.

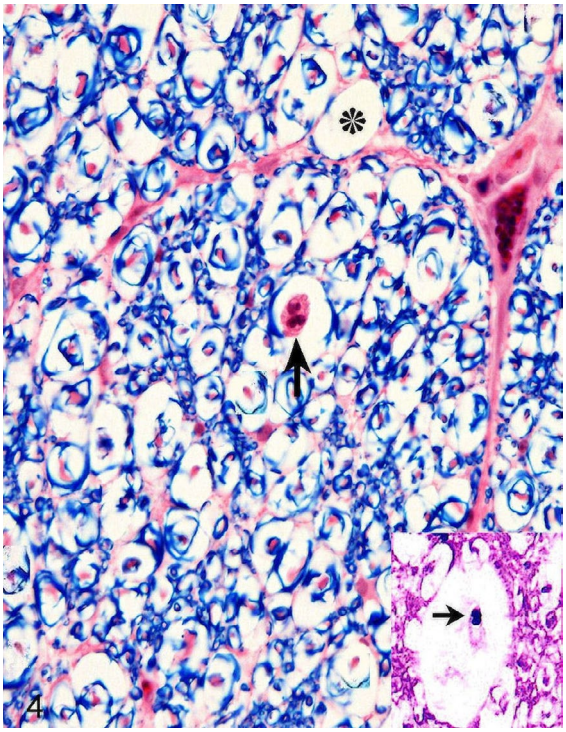

Figure 4 Spinal cord. Myelinated nerve fibers in the white matter show dilation of myelin sheath (asterisk) containing macrophage (arrow). LFB-HE. Inset: Macrophage within dilated myelin sheath exhibits nuclear pyknosis and dissolved cytoplasm (arrow). HE.

vacuole, were seen in the AF of 6 pigs. In 4 pigs (case Nos. 1-3, 5), they were recognized more often in the areas surrounding necrotic foci **(Figure 3)**. These chondrocytes stained positively with TUNEL assay, indicating apoptotic cell death **(Figure 3, inset)**. Apoptotic bodies were scattered adjacent to, or distant from, apoptotic chondrocytes. Neither microporous changes, necrotic lesions, nor apoptotic chondrocytes were observed in any of the control discs (n=6). Outer zones of the NP were unremarkable.

In the thoracic and lumbar spinal cord of all 6 pigs, a few myelinated nerve fibers in the white matter exhibited changes similar to Wallerian-type degeneration, with no evidence for tract specificity in the dorsal, lateral, or ventral funiculus. The incidence rate of degenerated nerve fibers was 3 to 7 per cross-sectional area of each spinal cord segment. Degenerated nerve fibers showed dilation of myelin sheaths with thinned or undetectable myelin lamellae in LFB-HE-stained sections. Dilated myelin sheaths were empty or contained macrophages **(Figure 4)**. Some macrophages exhibited degenerative features, such as pyknotic nuclei and cytolysis **(Figure 4, inset)**. Dilation of myelin sheaths was confirmed as such by strong immunoreactivity for MBP **(Figure 5)**. LFB-HE stain did not reveal any areas indicating deficit of stainable myelin in the white matter. There was no activation of astrocytes. Neurons in the gray matter horn were unremarkable. Alteration of myelinated nerve fibers was not observed in the control pigs.

The longissimus thoracis muscle of the 6 pigs exhibited the presence of a few slightly atrophied muscle fibers **(Figure 6)**. Such

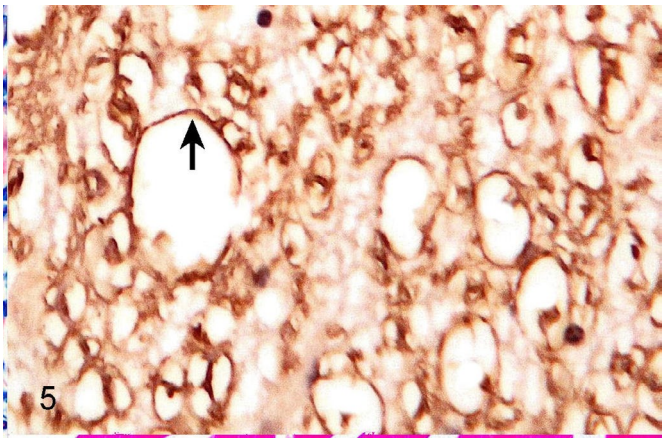

Figure 5 Spinal cord. A membrane lining dilated space of myelinated nerve fiber in the white matter represents an obvious increase in MBP stain intensity (arrow), indicating myelin sheath origin of the space. Immunohistochemical stain.

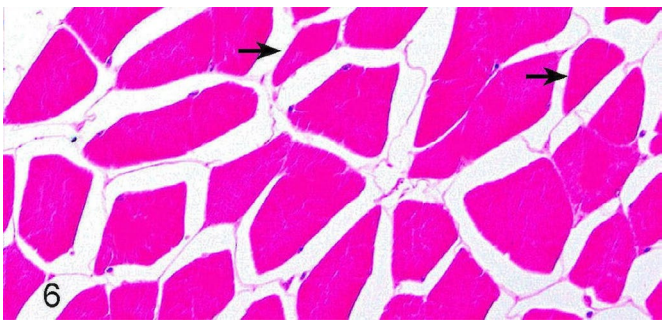

Figure 6 Skeletal muscle. Slightly atrophic muscle fibers (arrows) are seen in the longissimus thoracic muscle. HE.

fibers occurred sporadically, with no specific group atrophy or predilection for any muscle fascicle. Edema of the muscle spindle was rarely seen in 1 case (No. 2). Interstitial connective tissues showed mild edematous loosening. Intramuscular blood vessels and nerve bundles were unremarkable. To a lesser degree, muscle fiber atrophy was seen in 3 of the control pigs.

Discussion

Even though morphologic methods may cause artificial tissue damage to the IVD [17], the degenerative lesion in the AF of the present pigs was distinguished from the artificial product by the following reasons. First, macroscopically discolored annular areas related to the histopathologic lesions were differentiated from a postmortem alteration or artificial phenomenon. All IVDs were removed immediately after slaughter of animals. Second, in the area of microcavitation, all microcyst-like spaces were clearly demarcated from the surrounding annular tissue, and some contained collagenous tissue pieces exfoliated from the annular matrix, along with those elastic tissue elements, which could have partially been dissociated from the elastic fiber network that is specific for the annular matrix [19-22]. It is unlikely that some collagen/elastic fibers became separate from the annulus lamellae and got into the microcyst-like spaces, while sparing many other fibers, through the artifact process. Third, necrotic foci, which were composed of necrotic chondrocytes/collagen fibers, must be an acquired lesion that cannot be produced artificially. Last, both the microcavitation and focal necrosis were not found in those histologic sections of IVD, which were prepared for control pigs (n=6) with the same method as the 6 pigs with spinal deformity.

Usually in degenerated IVD tissue, deteriorated annulus lamellae may become fibrillated, fissured, bifurcated, and interdigitated [21,23,24], and the collagen/elastic fiber network become disorganized [24]. Precise pathophysiologic mechanism for the development of AF microcavitation, described here but not reported elsewhere, remains undetermined. However, this annular lesion probably resulted from partial degradation and loss of the annular matrix components (collagen/elastic fibers), as alluded to above. Appearance of this microcavitation may suggest that degradation of the extracellular matrix components occurred on a small scale but involved multiple sites of the AF, giving rise to polymicrocavitation. Identifying the involved collagen types (type I, type II, or other type collagen fibrils) [21,25] was unavailable in this study. Presumably, the lesion of microcavitation may have led to disengagement of proteoglycans and water binding to the annular matrix [21,24]. Although relatively uncommon, cyst-like spaces or pseudocysts may occur following damage to collagen/elastic fibers in those tissues that are richly endowed with collagen/elastic fibers, like the AF. A notable example is a human disorder of large arteries, particularly aortic aneurysm, which is pathologically termed cystic medial degeneration (necrosis) where fragmentation and loss of collagen/elastic fibers and degradation of extracellular elastin create cyst-like spaces within the vascular walls [26-28]. Two types of medial degeneration, microcystic or disseminated cystic, may occur in that vascular disorder [26].

Alternating angled and layered structure of the AF is ideal for withstanding large and complex loads in multiple directions, and structural changes affect mechanical properties of the AF [19]. In the present swine cases, it is assumed that the annular lesion, associated with compromised matrix quality and diminished mechanical properties [29], may have caused impaired adaptation of the AF tissues to compressive or tensile loads. However, it remains to be explained why the lesion of microcavitation in the AF involved more prominently those concentric lamellae that are oriented at the same angle. Occurring in 4 of the 6 pigs and involving collagen fibers and chondrocytes, another structural change – focal necrosis – may have also played a role in microstructural derangement of the AF. Apoptotic chondrocytes observed in the lesional AF have been previously described in mechanical overload- or trauma-induced IVD degeneration in humans, in which the mitochondrial apoptosis signaling pathway may mediate, promote, and amplify the disc changes [30,31]. Apoptosis is recorded in disc cells of porcine cervical spine that underwent traumatic injury [32]. Thus, apoptosis may have played an important role in the IVD degeneration, as has been demonstrated for many years [33].

It is considered that in the present study, the occurrence of AF lesion was linked intrinsically with kyphosis/lordokyphosis/lordosis, taking into account that the incidence of lesional AF, particularly microcavitation, was much higher (23/24, 95.8%) between deformed spinal regions than other regions (17/53, 32%) in the same pigs. In addition, the lesion of focal necrosis was of acute nature. These evidences may suggest that the AF lesion was a secondary event which followed the occurrence of spinal deformity. Given that cellular physiology in the IVD is strongly affected by mechanical loading [25], and excessive mechanical loading disrupts a disc's structure [34], the spinal deformity-induced physical stress to the IVD may be prospected. Although having pathologic images different from those of spinal deformity, spondylosis deformans or ankylosing spondylosis common in domestic animals such as pigs, bulls, and dogs may exhibit degenerative changes in the AF, which follow the development of osteophytes [18]. However, finally determining whether the AF lesion played a primary role in the development of the vertebral deformity or, conversely, it occurred secondary to mechanical overlord generated by the spinal deformity should await further investigation of the deformed vertebral bodies *per se*. Research into the cartilage endplate should be also taken into consideration, given that 1 of the present pigs exhibited synostosis.

To a minor extent, degeneration of myelinated nerve fibers was found in the spinal cord white matter of all 6 pigs. Degenerated myelin sheaths had no more axons, suggesting the involvement of both myelin sheaths and axons. The distribution pattern, extent, and degree of this nerve fiber alteration were clearly different from those described previously in pigs with spinal cord injury caused by IVD extrusion [35] and neurodegenerative disorders of nutritional, genetic, toxic, dysbaric, or infectious etiologies [36-40]. The current pigs were not associated with evident neurologic impairment antemortem, although subtle motor abnormalities cannot be ruled out. Hence, it is likely that such nerve fiber alteration did not reach a sufficiently distinctive degree to present

recognizable clinical sign, probably representing a subclinical lesion.

Having a phenotypic expression similar to some degree to that described here, occasional nerve fiber degeneration characterized by single, isolated chains of myelin ellipsoids occurs incidentally in an otherwise normal funiculus of the spinal cord in mature and aged domestic animals [41]. Furthermore, accumulating evidence indicates the presence of age-related alteration or loss of myelinated nerve fibers in the white matter of human and primate central nervous system [42-44]. The pathologic process in these instances is complex. For example, an abnormality of myelin sheaths, designated as myelin balloon, is recognized during aging [42]. On the other hand, the thinner myelinated nerve fibers are primarily lost with a relative preservation of the thicker ones [43]. Moreover, many myelinated nerve fibers degenerate and are lost, while in other myelinated nerve fibers only their sheaths degenerate, leaving the axons intact [44]. In domestic animals, the frequency of axonal swelling (spheroid formation) increases with age [22]. It should be noted that the participation of macrophages characteristic of Wallerian-type degeneration has scarcely been alluded to and depicted in the previously published studies on age-related regression of myelinated nerves, indicating that macrophage reaction is not necessarily implicated in such nerve fiber regression. Thus, the latter phenomenon possibly exhibits a histopathologic phenotype distinct from that reported in this study.

Aging would be an unlikely mechanism for the occurrence of myelinated nerve fiber degeneration in the pigs here (6 months old), even though the brain growth spurt in pigs starts prenatally and peaks around birth, similar to that in humans [45], and heterogeneous process of cerebral aging is associated with a high degree of inter-individual variability [46]. Alternatively, there is the likelihood that the nerve fiber alteration was what has been correlated with spinal deformity, considering that the control spinal cords were unremarkable. Although speculative, a possibility that the bending of spinal canal due to vertebral column deformity could have given mechanical damage (mild and persisting stretch) to myelinated nerve fibers in the spinal cord is raised. Indeed, an experimental study using *in vitro* model of axonal stretch revealed physiologic and anatomic damage to a small portion of myelinated axons in the white matter strips extracted from spinal cord [47]. Another experimental study using a recently developed compartmentalized *in vitro* model of primary cortical neurons [48] demonstrated that axonal degeneration following mild and repetitive stretch injury involves destabilization of the microtubule cytoskeleton of axons [49].

A small number of atrophic muscle fibers in the longissimus thoracis muscle were seen not only in the present 6 pigs but also in control muscles, indicating that the spinal deformity occurred in the absence of significant muscle failure.

It may be actually difficult to totally remove IVDs from live patients suffering from spinal deformities, so pathologic elucidation of *in vivo* structural changes in the discs from considerable length of the deformed spinal column is challenging. Because skeletally immature pigs closely model the human spine [11], the histopathologic findings observed in this small study may serve as a reference when studying deformities of the thoracic spinal column in humans.

Funding

The author received no financial support of the research, authorship, and/or publication of this article.

Competing Interests

The author declared no potential conflicts of interest with respect to the research, authorship, and/or publication of this article.

References

1 Bowen RE, Abel MF, Arlet V, Brown D, Burton DC, et al. (2012) Outcome assessment in neuromuscular spinal deformity. J Pediatr Orthop 32: 792-798.

2 Sitte I, Kathrein A, Pfaller K, Pedross F, Klosterhuber M, et al. (2013) Morphological differences in adolescent idiopathic scoliosis: a histological and urtrastructural investigation. Spine (Phila PA 1976) 38: 1672-1689.

3 Sparrey CJ, Bailey JF, Safaee M, Clark AJ, Lafage V, et al. (2014) Etiology of lumbar lordosis and its pathophysiology: a review of the evolution of lumbar lordosis, and the mechanics and biology of lumbar degeneration. Neurosurg Focus 36: E1.

4 Yamato Y, Matsuyama Y, Hasegawa K, Aota Y, Akazawa T, et al. (2017) A Japanese nationwide multicenter survey on perioperative complications of corrective fusion for elderly patients with adult spinal deformity. J Orthop Sci 22: 237-242.

5 Done SH, Greham ACJ (1986) Lordosis and kyphosis ("humpy-back") in pigs. Pig J 26: 128-135.

6 Holl JW, Rohrer GA, Shackelford SD, Wheeler TL, Koohmaraie M (2008) Estimates of genetic parameters for kyphosis in two crossbred swine populations. J Anim Sci 86: 1765-1769.

7 Lahrmann KH, Hartung K (1993) Causes of kyphotic and lordotic curvature of the spine with cuneiform vertebral deformation in swine. Berl Munch Tierarztl Wochenschr 106: 127-132.

8 Mirbagheri SS, Rahmani-Rasa A, Farmani F, Amini P, Nikoo MR (2015) Evaluating kyphosis and lordosis in students by using a flexible ruler and their relationship with severity and frequency of thoracic and lumbar pain. Asian Spine J 9: 416-422.

9 Scott P (2005) Scoliosis and other spinal deformities. In: Delisa JA, Gans BM, Walsh NE (eds.) Physical Medicine and Rehabilitation. 4th edn. Philadelphia, PA: Lippincott Williams & Wilkins, pp: 679-698.

10 Lindholm-Perry AK, Rohrer GA, Kuehn LA, Keele JW, Holl JW, et al. (2010) Genomic regions associated with kyphosis in swine. BMC Genetics 11: 112.

11 Nielsen LWD, HØgedal P, Arnbjerg J, Jensen HE (2005) Juvenile kyphosis in pigs. A spontaneous model of Scheuermann's kyphosis. Acta Pathol Immunol Scand 113: 702-707.

12 Patel A, Leven D, Lafage (2013) Animal models for spinal deformity and their role in the development of surgical nonfusion AIS

treatments. In: Sharan AD, Tang SY, Vaccaro AR (eds.), Basic Science of Spinal Diseases. New Delhi: Jaypee Brothers Medical Publishers, pp: 61-72.

13 Penny RHC, Walters JR (1986) A "humpy-back" syndrome of pigs. Vet Ann 26: 128-135.

14 Mulcahey MJ, Gaughan JP, Betz RR, Samdani AF, Barakat N, et al. (2013) Neuromuscular scoliosis in children with spinal cord injury. Top Spinal Cord Inj Rehabil 19: 96-103.

15 Protopsaltis TS, Boniello AJ, Schwab FJ (2016) Management of spinal deformity in adult patients with neuromuscular disease. J Am Acad Orthop Surg 24: 634-644.

16 Yu J, Fairbank JC, Roberts S, Urban JP (2005) The elastic fiber network of the annulus fibrosus of the normal and scoliotic human intervertebral disc. Spine 30: 1815-1820.

17 Friedmann A, Goehre F, Ludtka C, Mendel T, Meisel HJ, et al. (2017) Microstructure analysis method for evaluating degenerated intervertebral disc tissue. Micron 92: 51-62.

18 Palmer N (1993) Bones and joints. In: Jubb KVF, Kennedy PC, Palmer N (eds.), Pathology of Domestic Animals. 4th edn. San Diego, CA. Academic Press, pp: 1-181.

19 Guerin HAL, Elliott DM (2006) Structure and properties of soft tissues in the spine. In: Kurz SM, Edidin AA (eds.), Spine Technology Handbook. Amsterdam: Elsevier, pp: 35-62.

20 Smith LJ, Fazzalari NL (2009) The elastic fibre network of the human lumbar annulus fibrosus: architecture, mechanical function and potential role in the progression of intervertebral disc degeneration. Eur Spine J 18: 439-448.

21 Urban JP, Roberts S (2003) Degeneration of the intervertebral disc. Arthritis Res Ther 5: 120-130.

22 Youssef SA, Capucchio MT, Rofina JE, Chambers JK, Uchida K, et al. (2016) Pathology of the aging brain in domestic and laboratory animals, and animal models of human neurodegenerative diseases. Vet Pathol 53: 327-348.

23 Inoue N, Espinoza Orias AA (2011) Biomechanics of intervertebral disc degeneration. Orthop Clin North Am 42: 487-499.

24 Silberberg R (1977) Diseases of joints. In: Anderson WAD, Kissane JM, eds. Pathology. Saint Louis, MO: CV Mosby, 2015-2054.

25 Vergroesen PP, Kingma I, Emanuel KS, Hoogendoorn RJ, Welting TJ, et al. (2015) Mechanics and biology in intervertebral disc degeneration: a vicious circle. Osteoarth Cartlilage 23: 1057-1070.

26 Amalinei C, Caruntu ID (2013) Etiology and pathogenesis of aortic aneurysm. In: Amalinei C (ed.) InTech.

27 Ferraraccio F, Esposito S, Sante P, Cerasuolo F, Agozzino M, et al. (2004) Scanning electron microscopy of aortic medial changes in aortic ascending dilatation. Ultrastruct Pathol 28: 137-140.

28 Yuan SM, Jing H (2011) Cystic medial necrosis: pathological findings and clinical implications. Rev Bras Cir Cardiovasc 26: 107-115.

29 Cheng KK, Berven SH, Hu SS, Lotz JC (2014) Intervertebral discs from spinal nondeformity and deformity patients have different mechanical and matrix properties. Spine 14: 522-530.

30 Rannou F, Lee TS, Zhou RH, Chin J, Lotz JC, et al. (2004) Intervertebral disc degeneration: the role of the mitochondrial pathway in annulus fibrosus cell apoptosis induced by overload. Am J Pathol 164: 915-924.

31 Tschoeke SK, Hellmuth M, Hostmann A, Robinson Y, Ertel W, et al. (2008) Apoptosis of human intervertebral discs after trauma compares to degenerated discs involving both receptor-mediated and mitochondrial-development pathways. J Orthop Res 26: 999-1006.

32 Sitte I, Kathrein A, Pfaller K, Pedross F, Roberts S (2009) Intervertebral disc cell death in the porcine and human injured cervical spine after trauma: a histological and ultrastructural study. Spine (Phila Pa 1976) 34: 131-140.

33 Zhang F, Zhao X, Shen H, Zhang C (2016) Molecular mechanisms of cell death in intervertebral disc degeneration (review). Int J Mol Med 37: 1439-1448.

34 Adams MA, Roughley PJ (2006) What is intervertebral disc degeneration, and what causes it? Spine (Phila Pa 1976) 31: 2151-2161.

35 Lapointe JM. Summers BA (2012) Intervertebral disk disease with spinal cord penetration in a Yucatan pig. Vet Pathol 49: 1054-1056.

36 de Lahunta A (1983) Veterinary Neuroanatomy and Clinical Neurology. 2nd edn. Philadelphia, PA: WB Saunders.

37 Delgado F, Burtre C, Capellino F, Salvat A, Blanco Viera FJ (2011) Outbreak of ataxia in pigs associated with consumption of piquillin (*Condalia microphylia*). Vet Pathol 48: 803-806.

38 Dick EJ Jr, Broome JR, Hayward IJ (1997) Acute neurologic decompression illness in pigs: lesions of the spinal cord and brain. Lab Anim Sci 47: 50-57.

39 Jubb KVF, Huxtable CR (1993) The nervous system. In: Jubb KVF, Kennedy PC, Palmer N, eds. Pathology of Domestic Animals, 4th edn. San Diego, CA: Academic Press, pp: 267-439.

40 O'Toole D, Wells G, Ingram J, Cooley W, Hawkins S (1994) Ultrastructural pathology of an inherited lower motor neuron disease of pigs. J Vet Diagn Invest 6: 230-237.

41 Summers BA, Cummings JF, de Lahunta A (1995) Veterinary Neuropathology. St. Louis, MO: Mosby-Year Book, pp: 49-67.

42 Feldman ML, Peters A (1998) Ballooning of myelin sheaths in normally aged macaques. J Neurocytol 27: 605-614,

43 Marner L, Nyengaard JR, Tang Y, Pakkenberg B (2003) Marked loss of myelinated nerve fibers in the human brain with age. J Comp Neurol 462: 144-152.

44 Peters A (2009) The effects of normal aging on myelinated nerve fibers in monkey central nervous system. Front Neuroanat 3: 11.

45 Franz J, Van der Staay, Rebecca E (2017) Large farm animal models of human neurobehavioral and psychiatric disorders: methodological and practical considerations. In: Conn PM, (ed.) Animal models for the study of human disease, 2nd edn. London: Academic Press, pp: 72-102.

46 Gunning-Dixon FM, Brickman AM, Cheng JC, Alexopoulos GS (2009) Aging of cerebral white matter: a review of MRI findings. Int J Geriatr Psychiatry 24: 109-117.

47 Shi R, Pryor JD (2002) Pathological changes of isolated spinal cord axons in response to mechanical stretch. Neurosci 110: 765-777.

48 Yap YC, Dickson TC, King AE, Breadmore MC, Guijt RM (2014) Microfluidic culture platform for studying neuronal response to mild to very mild axonal stretch injury. Biomicrofluidics 8: 044110.

49 Yap YC, King AE, Guijt RM, Jiang T, Blizzard CA, et al. (2017) Mild and repetitive very mild axonal stretch injury triggers cytoskeletal mislocalization and growth core collapse. PLoS One 12: e0176997.